phys. stat. sol. (b) **188**, 493 (1995)

Subject classification: 71.35 and 78.47; S8.11; S8.12

Institut für Festkörperphysik der Technischen Universität Berlin[1])

Dephasing of Acceptor Bound Excitons in II–VI Semiconductors

By

B. LUMMER, R. HEITZ, V. KUTZER, J.-M. WAGNER, A. HOFFMANN, and I. BROSER

Degenerate four-wave-mixing experiments (DFWM) at the neutral acceptor bound exciton complex in CdS and ZnSe are reported. ps- as well as fs-spectroscopy are carried out to investigate the dephasing processes at this complex. The results are discussed concerning scattering of free excitons, phonons, and interactions with impurity centers. Higher orders of diffraction in the DFWM process are modeled within the density matrix equations for noninteracting two-level systems including propagation effects. From nonlinear quantum beat spectroscopy the binding energies of the acceptor bound biexciton in CdS and ZnSe are estimated.

1. Introduction

Four-wave mixing (FWM) has been proven as a powerful tool for the investigation of coherent dynamics in semiconductors (see, e.g. [1]). With spectrally selective ps-excitation dephasing times of some hundred ps are reported for bound exciton complexes in semiconductors, determined either by linear quantum beat spectroscopy [2] or by degenerate four-wave mixing [3, 4]. Extending the investigations to fs-experiments, a mixture of coherently excited states near the band gap of semiconductors is prepared, leading to complex interference effects [5].

Additionally, higher orders of diffraction have been observed in FWM experiments [6, 7]. Here, the occurrence of higher-order diffractions is explained with non-sinusoidal gratings. Recently, we reported on higher orders of diffraction induced by propagation effects in an optically dense medium of finite width [8].

In this contribution we want to report on degenerate four-wave-mixing experiments (DFWM) in the self-diffraction geometry at the neutral acceptor bound exciton complex (A^0, X) in CdS and ZnSe. First we consider its dephasing mechanisms investigated with ps-excitation and describe the second order of diffraction in CdS. Then we proceed to fs-excitation and emphasize on nonlinear quantum beats from the three-level system A^0, (A^0, X), and (A^0, M) in CdS and ZnSe. Here (A^0, M) denotes a biexciton M bound to the neutral acceptor.

2. Samples and Experimental Set-Up

The CdS samples used are nominally undoped platelets of about 15 μm thickness with the *c*-axis in the sample plane. They are selected for $\approx 30\%$ absorption at the (A^0, X)-resonance. The investigated ZnSe samples are high-quality p-type MBE-grown epilayers. The p-doping is performed with a nitrogen plasma source. The two samples presented here are 0.96 and 3.8 μm

[1]) Hardenbergstr. 36, D-10623 Berlin, Federal Republic of Germany.

thick with a net acceptor concentration of 3×10^{16} and 5×10^{15} cm^{-3}, respectively. The net acceptor concentration has been derived from CV profiling. For transmission experiments the ZnSe samples are glued onto quartz glass before the GaAs substrate is removed by selective wet chemical etching [9].

Monochromatic absorption measurements are performed dispersing the spectrum of a halogen lamp in a 0.75 m double grating monochromator before exciting the sample. For polychromatic absorption measurements the sample is illuminated by the whole spectrum of the halogen lamp and the transmitted light is dispersed in the monochromator.

Time-resolved luminescence is carried out by time-correlated single photon counting using a synchronously pumped dye laser (2 ps pulse width) as excitation source and a MCP photomultiplier in conjunction with a subtractive double monochromator.

For the ps-DFWM experiments in CdS the synchronously pumped dye laser has been used, too. All other DFWM measurements are performed with a frequency doubled passive mode-locked Ti:sapphire laser providing pulses of 1.5 ps or 150 fs pulse width optionally. The DFMW signal under spectrally selective ps-excitation is detected time-integrated by a photodiode in 'lock-in' technique and time-resolved with an MCP photomultiplier. With fs-excitation the DFWM signal is spectrally dispersed by a double monochromator and detected time-integrated by an optical multichannel analyzer (OMA).

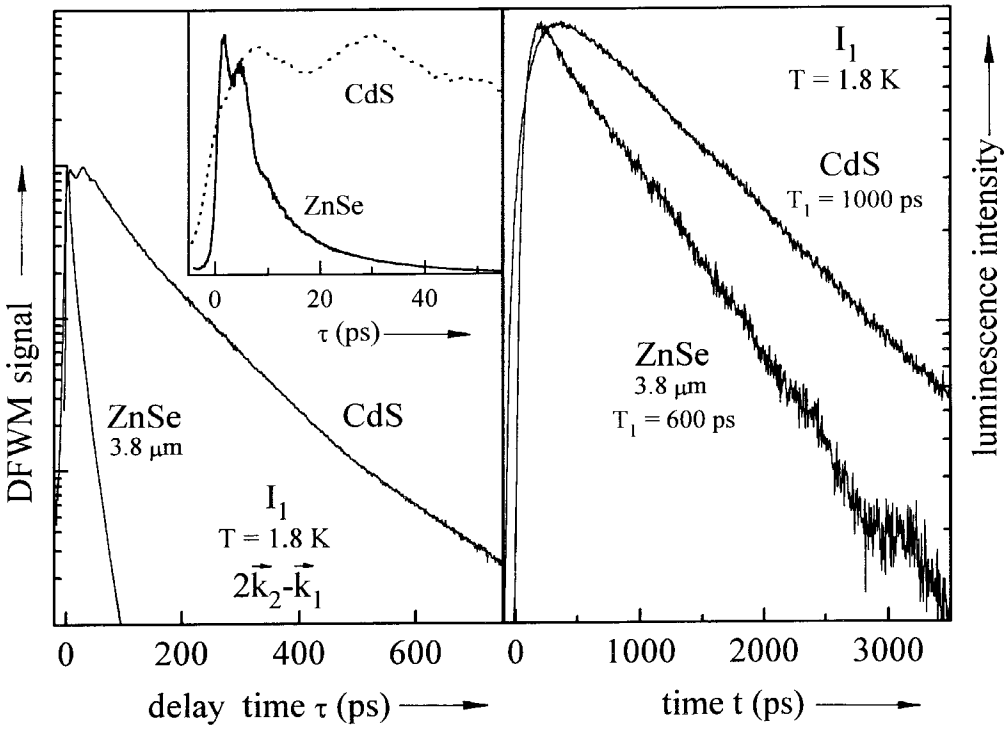

Fig. 1. DFWM (left part) and luminescence transients (right part) of the (A^0, X)-resonance under nonresonant ps-excitation in CdS and ZnSe. The inset shows DFWM transients on a linear scale clearly revealing the beat structure for short delay times

3. Experimental Results and Discussion

3.1 Dephasing of acceptor bound excitons

For a strongly localized system as the acceptor bound exciton in ZnSe or CdS one expects long dephasing times governed only by energy relaxation processes (T_1), giving $T_2 = 2T_1$.

For CdS and ZnSe we determined the energy relaxation time T_1 of the I_1 transition ($(A^0, X) \leftrightarrow A^0 + h\nu$) with time-resolved luminescence to 1000 and 600 ps, respectively (right part of Fig. 1). For the investigated samples DFWM experiments yield (left part of Fig. 1) a dephasing time T_2 of 800 ps in CdS and 70 ps in ZnSe for the (A^0, X)-complex. These values have been extracted from transients recorded at low excitation density and at low temperature using the fact that the transition is inhomogeneously broadened [10]. Interestingly, the dephasing time in the ZnSe samples is drastically decreased compared to CdS, although the energy relaxation times are nearly equal.

To get additional information on the dephasing mechanisms we measured the DFWM signal in dependence on temperature and excitation density in CdS. From the temperature dependence we concluded that at $T = 2$ K phonons do not influence the dephasing of the (A^0, X)-complex [10]. The dependence of the DFWM signal on the excitation density is depicted in Fig. 2. We observe a nonexponential decay of the transients for delay times up to 500 ps. At larger delays the signal becomes nearly exponential with a decay constant of about 200 ps independent of the excitation density.

A nonexponential decay of the DFWM transient indicates interaction with a time-dependent bath. To model the influence of a time-dependent bath on the DFWM signal, we introduce a time-dependent, phenomenological damping constant $\gamma = 1/T_2 + N \exp(-t/T_{\text{bath}})$ into the density matrix equations for an inhomogeneously broadened two-level system. T_2 is the intrinsic dephasing time ($\gamma_2 = 1/T_2$) of the two-level system, N represents a dimensionless density of the bath including the scattering cross-section, and T_{bath} gives its lifetime ($\gamma_{\text{bath}} = 1/T_{\text{bath}}$). Here, we make the assumption that the first exciting pulse generates the entire bath. For δ-like excitation pulses these equations are solved analytically giving

$$S(\tau) \propto \exp\left(-4\gamma_2\tau - 2N\,\frac{1 - e^{-2\gamma_{\text{bath}}\tau}}{\gamma_{\text{bath}}}\right) \tag{1}$$

for the time-integrated DFWM signal $S(\tau)$ at delay times long compared to the reciprocal inhomogeneous linewidth. The solid lines in Fig. 2 represent fits to the transients using (1). From the fit parameters we obtain a dephasing time around 800 ps, the bath density N nearly remains constant, and the lifetime of the bath increases with increasing excitation density from 160 up to 500 ps.

As phonons are excluded we propose free excitons to form the time-dependent bath, because these are mobile excitations with an appropriate lifetime. On the first view there are two problems connected with a bath of free excitons. First, one expects rather few free excitons to be generated under resonant excitation of (A^0, X)-complexes. Second, the lifetime T_{bath} does not correspond to the decay time (40 to 80 ps) of the exciton luminescence which we measured by time-resolved luminescence under weak excitation for our CdS samples.

The first problem is solved within the following consideration. In strongly compensated semiconductors the recharging of compensated (ionized) donors and acceptors offers an efficient generation channel for free carriers and therewith for excitons. Evidence for such a

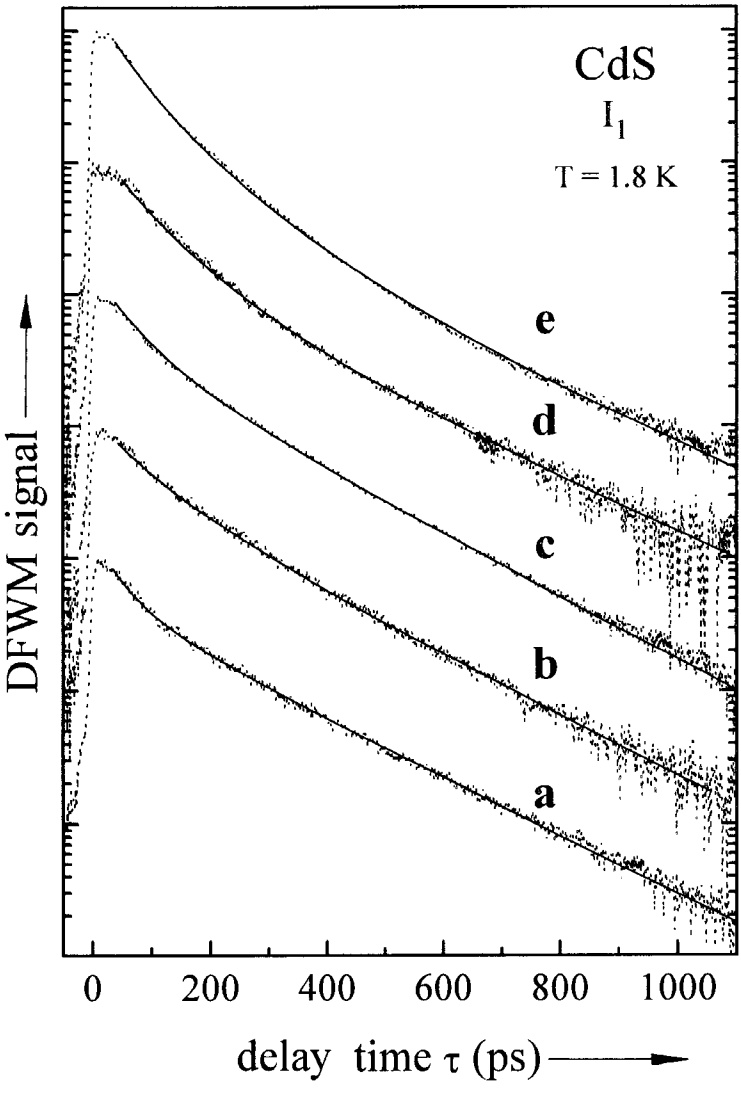

Fig. 2. DFWM transients at the (A^0, X)-resonance under ps-excitation in CdS for different excitation densities. The densities in MW/cm^2 are: (a) 1.0, (b) 1.5, (c) 2.0, (d) 2.5, and (e) 4.0

recharging is contained in Fig. 3, where mono- and polychromatic absorption spectra of a CdS and a ZnSe sample are depicted. The polychromatic excitation of the samples leads to a drastic increase of absorption in the bound exciton lines. We explain this with the increased number of neutral, shallow acceptors and donors recharged by photons with sufficient energy [11]. Further experiments show that the recharging of shallow defects is achieved by intense monochromatic excitation below the band gap, too. For example, the 'polychromatic' transmission spectra can be observed with a tunable dye laser.

In the investigated ZnSe samples a degree of compensation of about 65% is determined. With the known values of the net acceptor concentration at least 8×10^{16} and 1.4×10^{16} cm^{-3}

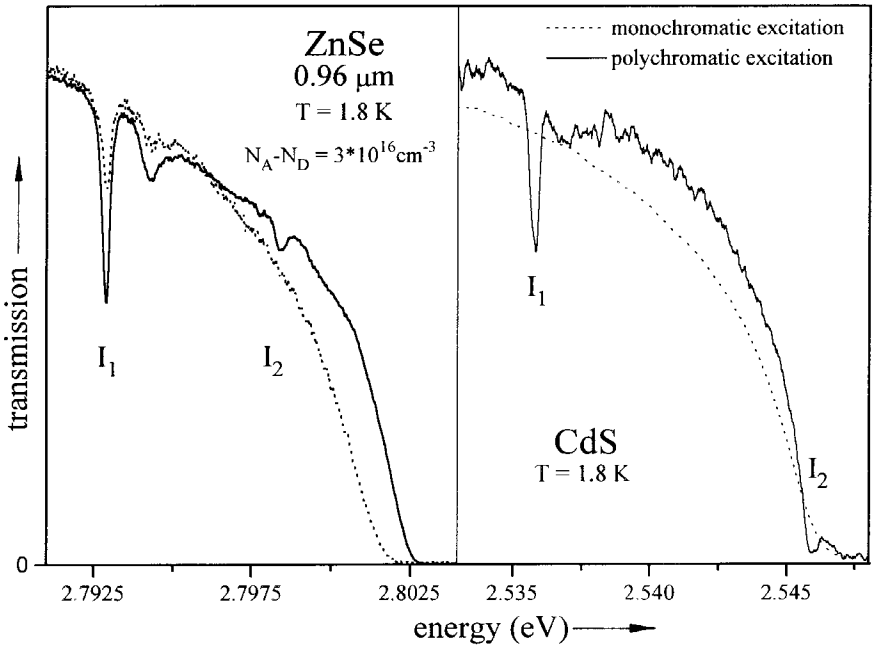

Fig. 3. Mono- and polychromatic recorded transmission spectra of a ZnSe epilayer (left part) and a CdS platelet (right part)

holes for the 0.96 and 3.8 μm samples and the same amount of free electrons is generated, respectively. So we find that the amount of generated free carriers is given by the density of compensated defects. In the CdS samples we have an orders of magnitude smaller amount of free carriers since these samples are not intentionally doped.

In a few ps these free carriers relax to the band edges where they are captured at deep centers or shallow defects or will form free excitons. The capture of free carriers at deep centers or shallow defects should not essentially affect the dephasing of bound exciton complexes, since they are immobile and captured for at least micro- or milliseconds. With a low density of deep defects as in our samples, there should be an efficient amount of free excitons generated by the recharging of shallow defects. These free excitons do affect the dephasing of the (A^0, X)-complex. Furthermore, here we see that the assumption of the first pulse creating the entire bath is reasonable, since its density is sufficient to recharge nearly all the compensated defects.

The problem of the lifetime of the free exciton bath is solved if we consider that at the used excitation densities the transmission spectra show higher transmission for the bound exciton lines indicating an effective saturation of the centers. Regarding trapping at defects as the main relaxation channel for free excitons, the increased lifetime of the exciton bath may be explained with the saturation of this recombination channel. This means, the saturation of recombination channels leads to prolonged lifetimes of free excitons. Indeed, we found anti-Stokes luminescence near the neutral donor bound exciton in CdS upon resonant excitation of the (A^0, X)-complex at high excitation densities.

The fits obtained with the 'bath' model (1) explain the nonexponential decay of the DFWM transients for short delay times. Since more free carriers and therewith more free

excitons are generated in the p-doped ZnSe epilayers the dephasing is accelerated compared to CdS. As the bath recovers the transients become nearly exponential with a dephasing time of 800 ps in CdS. To account for the fact of $T_2 \ll 2T_1$, we propose impurity interactions as dominant dephasing mechanism. This holds especially for the ZnSe samples with their higher absolute defect concentration. To conclude this subsection, we point out that the shortened dephasing times of the (A^0, X)-complex observed in our ZnSe samples are due to the high degree of compensation and the high absolute defect concentration.

3.2 The second-order diffracted signal

In the previous section, we showed that the 'intrinsic' dephasing time of the (A^0, X)-complex in our CdS samples amounts to 800 ps. This time is too short to be explained by energy relaxation. A decrease in the decay time of the DFWM transients with increasing optical density has been observed for the naphthalene impurity in pentacene [12]. This decrease has been explained with the influence of the optical density on the propagation of the electric field through the crystal. Recently, we showed that beside optical density effects the propagation of the electric field results in the occurrence of higher orders of diffraction [8]. Thus, the investigation of higher-order diffracted signals gives more insight into the generation process of the DFWM signal.

The left part of Fig. 4 compares the time-integrated DFWM signal in first ($2\boldsymbol{k}_2 - \boldsymbol{k}_1$) and second ($3\boldsymbol{k}_2 - 2\boldsymbol{k}_1$) orders of diffraction. Both signals are recorded simultaneously exciting the I_1 absorption in CdS. We observe some remarkable features in the transients.

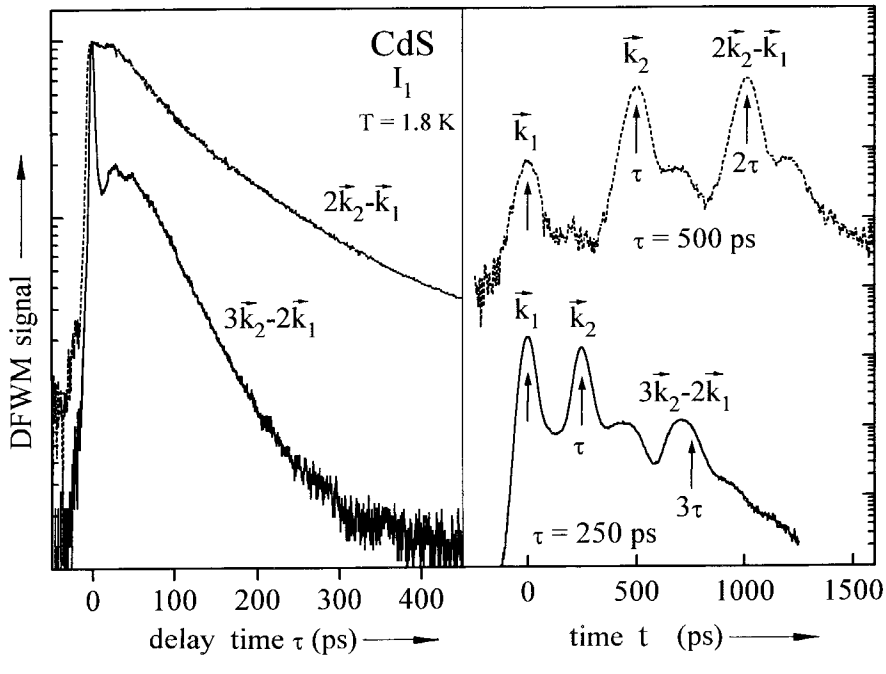

Fig. 4. Time-integrated (left part) and time-resolved (right part) DFWM signals in first ($2\boldsymbol{k}_2 - \boldsymbol{k}_1$) and second ($3\boldsymbol{k}_2 - 2\boldsymbol{k}_1$) order of diffraction recorded at the (A^0, X)-resonance in CdS. The time-integrated transients are normalized to the same maximum value

The decay of the transient in first order is nonexponential, but it becomes almost monoexponential for long delay times, as discussed in Section 3.1. The second order of diffraction shows a correlation peak at zero delay and the signal decays approximately 2.5 times faster than in first order. The right part of Fig. 4 compares time-resolved the diffracted signals. In first order the photon echo occurs a few ps before 2τ and its temporal width is caused by the time resolution of the experimental set-up. In contrast, in second order the photon echo has its maximum approximately 45 ps before 3τ and is considerably broader than the experimental resolution. A temporal width of 80 ps is estimated for the echo pulse in second order of diffraction.

3.2.1 Modeling of the second order of diffraction

In [7] the occurrence of higher orders of diffraction has been explained by higher Fourier components of the induced free carrier grating caused by diffusion and a period doubling of the grating due to the enhanced formation of excitons in regions of less free carrier density.

Here, we will explain the occurrence of higher orders of diffraction with propagation effects in an optically dense system of finite width. The investigated neutral acceptor bound exciton complex (A^0, X) represents a localized excitation in CdS. Its Bohr radius is orders of magnitude smaller than the mean distance between acceptor sites. Thus, to model our results we consider a noninteracting, inhomogeneous ensemble of statistically distributed two-level systems which are described by the density matrix equations. For simplicity, we neglect here the dephasing by the free exciton bath discussed in Section 3.1.

The propagation of the electric field is accounted for by Maxwell's wave equation. With the slowly-varying envelope approximation and in case of samples which are small compared to the extension of the excitation pulse and with moderate absorption we find a linear correction of the driving field E_0 in the density matrix equations [8],

$$E_0 = E_{\text{in}} + i \frac{\hbar}{\mu} L \langle \psi \rangle . \tag{2}$$

Here μ is the dipole matrix element of the transition and $\langle \psi \rangle$ is the polarization averaged over the inhomogeneous distribution. The coupling parameter

$$L = \frac{d}{4\pi} \int \alpha(\omega)\, \mathrm{d}\omega , \tag{3}$$

with the sample thickness d can be determined from the linear absorption. The density matrix equations are then solved numerically for finite pulse widths. The signals diffracted in various directions are separated by a Fourier transformation with respect to the relative phase of the incoming pulses.

The values for L and the inhomogeneous width of the lines have been deduced from the polychromatic transmission spectrum of the CdS sample. The damping constants for polarization and population are taken from our time-resolved experiments yielding $T_2 = 800$ ps and $T_1 = 1000$ ps (Section 3.1). The calculations shown in Fig. 5 reproduce the basic experimental features depicted in Fig. 4. The time-integrated signal decays faster in second than in first order and shows a correlation peak at zero delay. The time-resolved photon echo appears about 12 ps before 3τ having a FWHM of 75 ps instead of 50 ps as in first order. The polarization beats (Section 3.3) in the real time signal are not resolved in our experiments due to the limited experimental resolution.

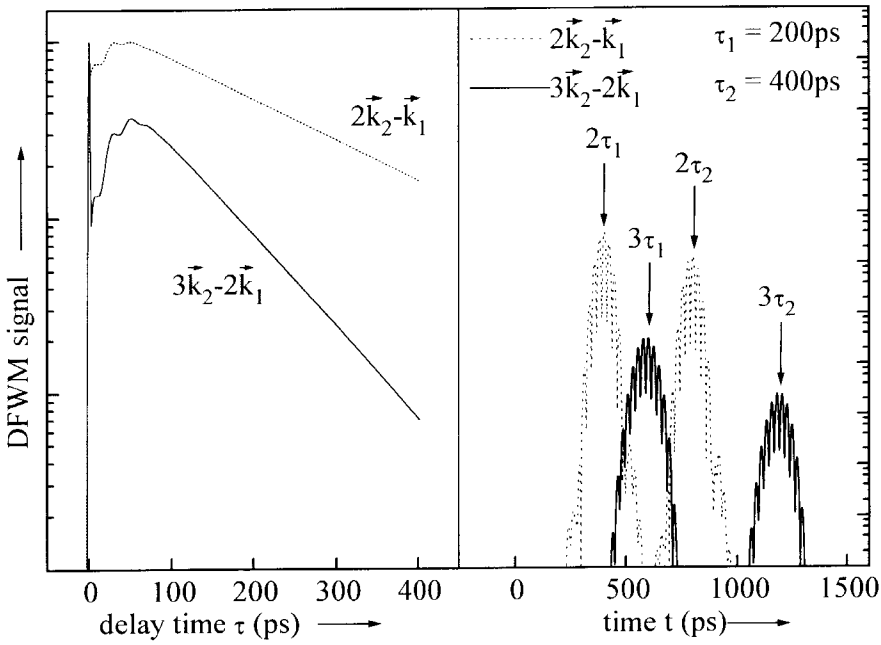

Fig. 5. Time-integrated (left part) and time-resolved (right part) DFWM signals in first ($2\boldsymbol{k}_2 - \boldsymbol{k}_1$) and second ($3\boldsymbol{k}_2 - 2\boldsymbol{k}_1$) order of diffraction calculated for independent two-level systems. The time-integrated transients are normalized to the same maximum value

In our model the appearance of higher-order diffracted signals is caused by the propagation induced cross-talk between the absorbing centers. The second diffracted order can be interpreted as the diffraction of the first-order signal at the grating generated by the incoming pulses. The polarization with wave vector $2\boldsymbol{k}_2 - \boldsymbol{k}_1$ 'inherits' the grating vector $\boldsymbol{k}_2 - \boldsymbol{k}_1$ and establishes a polarization with wave vector $3\boldsymbol{k}_2 - 2\boldsymbol{k}_1$. This is basically a DFWM process in the stimulated photon echo geometry leading to a photon echo at 3τ in the second order of diffraction. In a similar way it is obvious that in the n-th order of diffraction the echo occurs at $(n + 1)\,\tau$. In fact, the photon echo is found to appear earlier in both orders monitored. This is easily explained with the strong shaping of the echo pulse with the polarization decay. The shift in the second order deduced from our model is only 12 ps instead of the measured 45 ps for $T_2 = 800$ ps. We attribute this to the enhanced shaping of the echo pulse by the fast nonexponential polarization decay (Section 3.1) that is not treated in this model.

Since both signals are measured in dependence on τ the second-order diffracted signal decays faster due to the increased delay of the photon echo. Here, one expects a decay time of $T_2/8$. Interestingly we find a decay time of approximately $1/2.5 \cdot T_2/4 = T_2/10$ for both the calculated and measured signals in the second order of diffraction. This is due to the stimulated geometry in the DFWM process. The population grating which diffracts the '$2\boldsymbol{k}_2 - \boldsymbol{k}_1$' polarization into the $3\boldsymbol{k}_2 - 2\boldsymbol{k}_1$ direction decays with T_1, thus the decay time depends not only on T_2 but also on T_1. An expression for the decay time of the second-order diffracted signal may be derived from the analysis of the fifth order density matrix element under

the perturbation approximation [13]. We find a decay time of $(8/T_2 + 2/T_1)^{-1}$ for the second-order diffracted signal. For our system with a measured decay of $T_2/10$ this results in $T_2/T_1 = 1$ corresponding well to the value of 800 ps/1000 ps = 0.8 deduced from the first-order diffracted signal for long delay times and the luminescence decay time.

Our model considering a linear correction of the driving field E_0 has been checked by comparing the numerical results with the correct treatment of pulse propagation through the sample. We found that it holds up to a peak absorption of about 40% in the investigated transition. This exceeds our peak absorption of about 30%, indicating that we have measured the 'correct' dephasing time and may neglect the influence of optical density for the observed decay constant of the DFWM signal in CdS. In principle one has to be careful in extracting the dephasing time T_2 from DFWM experiments at systems with high optical density, as they are found for example near the band gap of semiconductors. Furthermore, in our model the population grating established by the incoming pulses exhibits no higher Fourier components – it is a sinusoidal grating – confirming the interpretation of the second order of diffraction as a pure propagation effect. Details of this treatment will be given in a forthcoming paper.

3.3 The (A^0, M)-complex

In Sections 3.1 and 3.2 we have studied the DFWM signal under spectrally selective ps-excitation. The spectrally narrow laser pulse excites only close-lying energy levels resulting in long beat periods in the DFWM transients. This is demonstrated in the inset of Fig. 1, showing modulations in the DFWM signal for CdS and ZnSe. For CdS we find a beat period of 23 ps corresponding well to the energy separation of 175 μeV between the bound exciton lines formed at two different neutral acceptors present in our samples. For ZnSe we find a beat period corresponding to the energy separation of 920 μeV between the ground state and one excited state of the (A^0, X)-complex (Fig. 3). In both cases, the ps-pulse excites both of the close-lying levels. According to their origin, we attribute the modulations to polarization interference and quantum beats in CdS and ZnSe, respectively.

With fs-excitation the broad laser pulse prepares a mixture of coherently excited states at the entire band gap of the investigated semiconductor. In general, this gives rise to a manifold beat pattern in the FWM signal. This kind of spectroscopy is referred to as nonlinear quantum beat spectroscopy (NQBS) [5].

Here, we want to present NQBS with fs-excitation at the neutral acceptor bound exciton in ZnSe and CdS. In Fig. 6a the linear transmission of a 3.8 μm ZnSe sample and the spectrum of the exciting fs-pulse are compared. The linear transmission resolves the resonance of the free exciton X and resonances of excitons bound to the neutral nitrogen acceptor I_1^N and to a neutral donor I_2. Fig. 6b gives the DFWM signal in dependence on τ recorded at the I_1^N resonance showing a rich beat pattern in the transient. In order to find the polarizations taking part in the observed beats one extracts the beat energies by a Fourier transformation of the transient. The beat energies then give the energy distance to the involved polarizations (Fig. 6c).

Since the observed beat pattern and the diminished dephasing time with fs-excitation have been discussed in [14], we want to concentrate on the I_1^M resonance. Fig. 7 shows the transients recorded for different detunings δE from the I_1 in CdS and ZnSe. In both cases the observed beats show no phase shift passing through the resonance indicating that the beating polarizations possess a common state [15]. This means, both of them are established

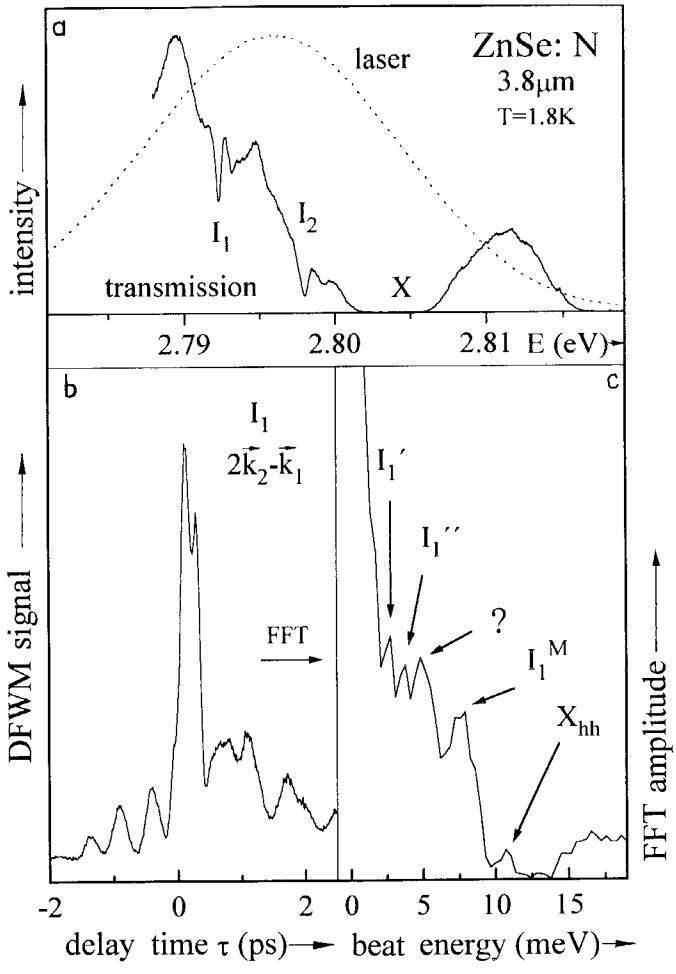

Fig. 6. DFWM signal recorded at the (A^0, X)-resonance under fs-excitation in ZnSe. For explanation see text

at the A^0-center. Following the results in CdSe [5] we propose a beating between the $A^0 \leftrightarrow (A^0, X)$ and the $(A^0, X) \leftrightarrow (A^0, M)$ polarizations. To illustrate this, Fig. 8 shows a term scheme for the free biexciton (right part) and the biexciton bound to an impurity center. The beating polarizations are established by the electric field of the incoming pulses between ground state and intermediate level and intermediate level and upper level in both cases. If quantum beats of the polarizations are observed, their common state has to be initially occupied as has been shown in [15]. Accordingly, the first excitation pulse establishes both, a population of (A^0, X)-complexes and the beating polarizations. The second pulse then gives rise to a polarization emitting in direction $2\boldsymbol{k}_2 - \boldsymbol{k}_1$ where the beats can be observed.

The beat energies observed in the DFWM experiments are $E^{\text{beat}} = E_x - E_m$ and $E_c^{\text{beat}} = E_{mc} - E_{xc}$ for the free and the bound biexciton, respectively (Fig. 8). We determine the binding energy of the bound biexciton from the beat energy according to

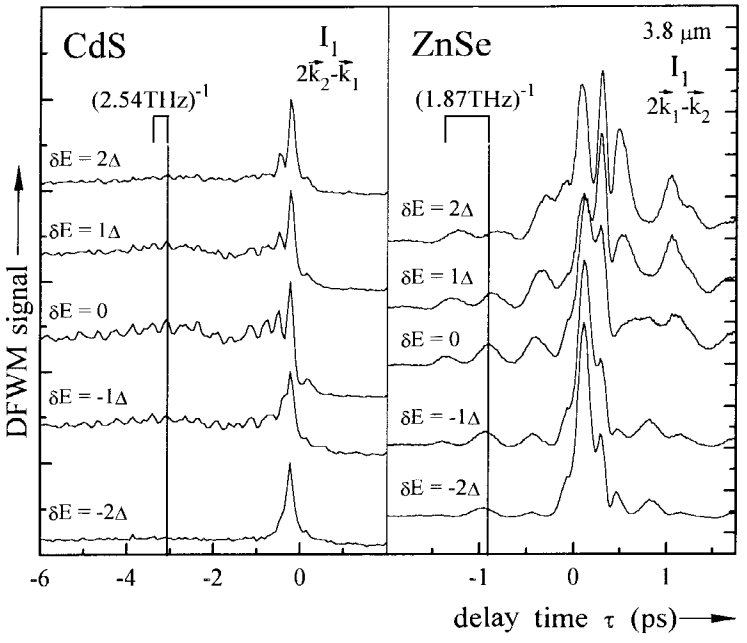

Fig. 7. DFWM signal recorded for different detunings from the (A^0, X)-resonance under fs-excitation in CdS and ZnSe. The detuning is Δ = 110 μeV for CdS and Δ = 140 μeV for ZnSe

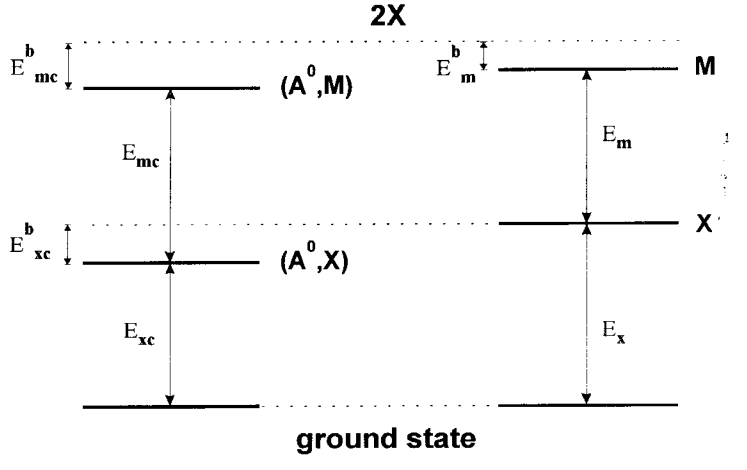

Fig. 8. Term scheme for the free biexciton (right part) and the biexciton bound to an impurity center A^0 (left part). E_x transition energy of the free exciton, E_m energy between the free biexciton state and the free exciton state, E_{xc} transition energy of the exciton bound to the A^0-center, E_{mc} transition energy between the bound biexciton and the bound exciton, E^b_m binding energy of the free biexciton, E^b_{mc} binding energy of the biexciton bound to the A^0-center, E^b_{xc} binding energy of one exciton bound to the A^0-center

Table 1
Comparison of beat and binding energies of the (A^0, M)-complex in II–VI semiconductors

	CdSe	ZnSe	CdS
E_c^{beat} (meV)	5.4 [17]	7.7	10.5
E_{xc}^b (meV)	8.3 [17]	10.5	17.7
E_{mc}^b (meV)	11.2	13.3	24.9
$E_{mc}^b - E_{xc}^b$ (meV)	2.9	2.8	7,2

$E_m^b = 2E_x - E_m - E_x = E^{beat}$ and $E_{mc}^b = 2E_x - E_{mc} - E_{xc} = 2E_{xc}^b - E_c^{beat}$, where E_{xc}^b just gives the binding energy of one exciton to the impurity center. So, in contrast to what is stated in [5], the binding energy of the biexciton bound to the impurity center is not $E_{mc}^b = E_c^{beat}$. The term scheme also shows that we define the binding energy of the (A^0, M)-complex with respect to the state formed by two free excitons. From the data given in [5] and our results on ZnSe and CdS we may extract the binding energy E_{mc}^b for the neutral acceptor bound biexciton (A^0, M) (Table 1). The beat energy of $E_c^{beat} = 10.5$ meV for CdS corresponds well to the energy separation of ≈ 11 meV between the I_1^M and I_1 luminescence that we extracted from the spectra presented in [16]. Table 1 shows that in the investigated semiconductors the binding energy of the second exciton to the impurity complex is smaller than the binding energy of the first exciton. The ratio $(E_{mc}^b - E_{xc}^b)/E_{xc}^b$ ranges between 30% and 40%.

It should be mentioned that here we assume the excited upper level to represent the lowest energy state of the (A^0, M)-complex. This assumption has to be discussed in the future in view of recent results [17] leading to the identification of two excited states for the (A^0, M)-complex in CdSe. One has to discuss the electronic structure of the (A^0, M)-complex and therewith the selection rules and oscillator strengths of the transitions.

4. Conclusion

In this contribution we have presented manifold experiments at the acceptor bound exciton in CdS and ZnSe in order to gain insight into their coherent and incoherent dynamics.

Energy relaxation processes have been investigated by time-resolved luminescence yielding $T_1 = 1000$ and 600 ps for the (A^0, X)-complex in CdS and ZnSe, respectively. With DFWM measurements their dephasing times have been found to amount to $T_2 = 800$ ps in CdS and $T_2 = 70$ ps in ZnSe for the investigated samples. These times have been determined for low excitation densities and low temperatures. The dephasing processes of the (A^0, X)-complex have been discussed regarding interactions with free excitons and impurities. These are responsible for the nonexponential decay of the transients and the shortened dephasing time compared to the energy relaxation time. Evidence for the generation of free excitons under resonant excitation of the acceptor bound exciton complex has been found by poly- and monochromatic transmission measurements, where the effective recharging of compensated shallow defects was demonstrated.

With the investigation of the second-order diffracted DFWM signal we gained further insight into the DFWM process. The experimental findings are well described within our model. The occurrence of higher-order diffracted signals is explained by propagation effects in an optically dense system of finite width. In principle, higher-order diffracted signals should be observable in any absorbing medium.

Extending the investigations to broad-band fs-excitation, quantum beats in the three-level system A^0, (A^0, X), and (A^0, M) have been observed. The binding energies of the (A^0, M)-complexes have been determined to $E^b_{mc} = 24.9$ and 13.3 meV in CdS and ZnSe, respectively. The spectrally broad fs-excitation offers the possibility to study even widely separated energy levels.

Acknowledgements

We are indebted to R. Zimmermann for very fruitful discussions and his cooperation. The authors are grateful to D. Hommel and E. Kurtz for providing the ZnSe epilayers. This work has been supported by the Deutsche Forschungsgemeinschaft.

References

[1] E. O. Göbel, Festkörperprobleme **30**, 269 (1990).
[2] H. Stolz, V. Langer, E. Schreiber, S. Permogorov, and W. von der Osten, Phys. Rev. Letters **67**, 697 (1991).
[3] H. Schwab, V. G. Lyssenko, and J. M. Hvam, Phys. Rev. B **44**, 3999 (1991).
[4] I. Broser, B. Lummer, R. Heitz, and A. Hoffmann, J. Crystal Growth **138**, 809 (1994).
[5] K. H. Pantke and J. M. Hvam, Internat. J. mod. Phys. B **8**, 73 (1994).
[6] H. Kalt, V. G. Lyssenko, R. Renner, and C. Klingshirn, J. Opt. Soc. Amer. B **2**, 1188 (1985), and references therein.
[7] H. Saito and E. O. Göbel, Optics Letters **11**, 354 (1986).
[8] R. Heitz, B. Lummer, J.-M. Wagner, A. Hoffmann, I. Broser, and R. Zimmermann, Proc. 22nd Internat. Conf. Physics of Semiconductors, Vancouver 1994, World Scientific Publ. Co., Singapore, to be published.
[9] N. Presser, G. Kudlek, J. Gutowski, S. M. Durbin, D. R. Menke, M. Kobayashi, and R. L. Gunshor, phys. stat. sol. (b) **159**, 443 (1994).
[10] R. Heitz, B. Lummer, A. Hoffmann, and I. Broser, J. Lum. **58**, 237 (1994).
[11] R. Heitz, B. Lummer, V. Kutzer, D. Wiesmann, A. Hoffmann, I. Broser, E. Kurtz, S. Einfeldt, J. Nürnberger, B. Jobst, D. Hommel, and G. Landwehr, Proc. Europ. Workshop II–VI Semiconductors, Linz (Austria) 1994, to be published in Mater. Sci. Forum.
[12] R. W. Olson, H. W. H. Lee, F. G. Patterson, and M. D. Fayer, J. chem. Phys. **76**, 31 (1982).
[13] T. Yajima and Y. Taira, J. Phys. Soc. Japan **47**, 1620 (1979).
[14] A. Hoffmann, B. Lummer, V. Kutzer, L. Eckey, R. Heitz, I. Broser, E. Kurtz, J. Nürnberger, B. Jobst, D. Hommel, and G. Landwehr, see [11].
[15] J. Erland and I. Balslev, Phys. Rev. A **48**, R1765 (1993).
[16] B. S. Razbirin and D. K. Nelson, Soviet Phys. – J. exper. theor. Phys., Letters **56**, 291 (1992).
[17] J. Erland, B. S. Razbirin, V. G. Lyssenko, K.-H. Pantke, and J. M. Hvam, J. Crystal Growth **138**, 800 (1994).

(Received November 7, 1994)